Jpn. J. Cancer Res. 82, 676–685, June 1991

Epigenetic Control of Tumor Cell Morphology

Keizo Horio,[1,5] Hiroshi Yoshikura,[1] Masahiro Kawabata,[1] Takashi Odawara,[1] Katsuko Sudo,[2] Yohei Fujitani,[3] Ganghong Lee[4] and Aikichi Iwamoto[1,6]

[1]Department of Bacteriology, Faculty of Medicine, University of Tokyo, 7-3-1 Hongo, Bunkyo-ku, Tokyo 113, Departments of [2]Laboratory Animal Research Center and [3]Fine Morphology, Institute of Medical Science, University of Tokyo, 4-6-1 Shirokanedai, Minato-ku, Tokyo 118 and [4]Department of Pathology, Cancer Institute, 1-37-1 Kami-Ikebukuro, Toshima-ku, Tokyo 170

XC cell line derived from a single rat cell transformed by the Prague strain of Rous sarcoma virus produced morphologically different colonies. Among them, two distinct cell types consisting of thick, fusiform cells (L-type), and of flat, polygonal cells (R-type) were apparent. By repeated subclonings, pure cultures, L1 and R1, respectively, were obtained. These clones underwent morphological conversion during prolonged culture; L-type colonies appeared in the R-type clone and *vice versa*. The kinetic curve suggested that the conversion was multi-stepped. When inoculated into nude mice, L-type cells produced much larger tumors at a higher frequency than R-type cells, and the tumors induced by these two clones were histologically different. The expression of v-*src* gene was higher in L-type than in R-type cells at both mRNA and protein levels.

Key words: XC cells — Morphological conversion

The morphology of mammalian cells cultured *in vitro* is fascinatingly various. Even a cloned cell line comes to contain various types of cells after prolonged culture. This phenomenon is so frequently encountered by those who work with cell culture that its significance has not seriously been questioned. Indeed, the shape of cells is often influenced by culture conditions such as the medium, the substrate where cells are growing and so on. However, freshly cloned cells show relatively stable morphology under the same culture conditions, at least for a certain period of time. Our understanding of the molecular basis of the cellular morphology is only partial, and we know little of how the cellular morphology is maintained and how the morphological variation is produced.

XC cell line is a clonal line established from a Wistar rat tumor induced by the Prague strain of Rous sarcoma virus (RSV).[1] Cultures of XC cells consist of a mixture of morphologically different cells. Two distinct types of colonies were present; those consisting of flat, non-refractile "blebby" cells (R-type) and those consisting of long, fusiform cells (L-type). These cells were not only different in morphology but also in the adenylyl cyclase system, particularly in the interaction between the catalytic unit and the α subunit of the stimulatory G proteins.[2] This paper deals with experiments which led us to the isolation of these cellular variants and reports an interconversion of the cellular morphology produced probably by epigenetic events.

[5] Present address: Department of Pediatrics, Faculty of Medicine, University of Tokyo, 7-3-1 Hongo, Bunkyo-ku, Tokyo 113.

[6] To whom correspondence should be addressed.

MATERIALS AND METHODS

Cell culture XC cell line was obtained from the late Dr. W. P. Rowe (National Institute of Allergy and Infectious Diseases, National Institutes of Health, USA). Rat fibroblastic cell line 3Y1 was obtained from Dr. K. Oda (Science University of Tokyo). H21, a clone of 3Y1 transformed by SRD strain of RSV, chick embryo fibroblasts (CEF) and SRA strain of RSV were obtained from the late Dr. S. Kawai (Institute of Medical Science, University of Tokyo). Cells were grown in Dulbecco's modified Eagle's minimal essential medium (DMEM, GIBCO Laboratories, Life Technologies, Inc., Grand Island, NY) supplemented with 7% fetal calf serum (HyClone Laboratories, Logan, UT). Cell cloning was performed by means of the cylinder technique.[3] L1 (R1) was established through multiple rounds of subcloning. L1r (R1r) was a direct subclone of L1 (R1), and LK1 (RK1), which we described previously,[2] is a direct subclone of L1r (R1r). Since the morphological stability of each subclone was not permanent (see below), frozen aliquots were made soon after subcloning and thawed periodically for use. Parental XC cell line, L-type and R-type subclones were free from mycoplasma. To examine the anchorage independence, cells were grown in 0.8% methyl cellulose (Sigma, St. Louis, MO) over a 1% agar basal layer.

Fluorescence staining of cells XC cells grown on coverslips were rinsed briefly in phosphate-buffered saline (PBS), fixed for 10 min in 3.7% formaldehyde in PBS at room temperature and washed extensively in PBS. After fixation, cells were dehydrated in absolute acetone for

4 min at −20°C and air-dried. To stain F-actin, rhodamine-conjugated phalloidin (Molecular Probes, Inc., Junction City, OR) was used as described.[4] Indirect immunofluorescence staining was performed as described[5] using monoclonal antibodies for vinculin (Bio Yeda, Israel) or for $p60^{src}$ (Oncogene Science Inc., Mineola, NY) as primary antibodies and fluorescein-conjugated anti-mouse IgG (MBL, Nagoya) as the secondary antibody.

Tumorigenicity on nude mice Cells were inoculated subcutaneously at a single site on the back of adult BALB/$c^{nu/nu}$ mice. The size of the tumors was measured after two weeks. Tumors were excised and divided into two pieces under sterile conditions. A piece of the tumor was fixed in PBS containing 3.7% formaldehyde and was examined histologically. The other piece was minced and replated in culture dishes to examine the morphology of the recovered cells.

Southern blot analysis High-molecular-weight DNA was extracted from the cells essentially as described.[6] This DNA (10 μg) was digested with restriction enzymes according to the recommendations of the supplier. Digested DNA was electrophoresed through agarose gels. After electrophoresis, gels were stained with 1 μg/ml of ethidium bromide, depurinated with 0.2 *M* HCl for 15 min, denatured, neutralized and blotted onto Nitro plus 2000 (Micron Separations Inc., Westborough, MA) as described.[7] The filters were baked for at least 2 h at 80°C under vacuum. The filters were hybridized with the probe for over 16 h at 65°C. The filters were washed with 1×SSC (0.15 *M* sodium chloride, 0.015 *M* sodium citrate) at 65°C and were exposed to Fuji RX films with intensifying screens. The molecular probes used for Southern blot analysis were RSV-LTR, five murine homeobox genes and the human β-actin promoter. RSV-LTR was *Nde* I-*Hin*d III fragment from RSV-CAT,[8] which consisted of about 520 bp from RSV (containing its 3′-LTR) and about 50 bp from pBR322.[9] DNA clones containing murine Hox-1.1 cDNA, murine genomic Hox-1 cluster on chromosome 6 and Hox-2 cluster on chromosome 11 were kindly provided by Dr. N. Takahashi (Department of Molecular Biology, School of Medicine, Nagoya University). These DNA clones were digested with the restriction enzymes indicated below and were purified by agarose gel electrophoresis. Hox-1.1 probe was *Sac* I-*Eco* RI fragment of Hox-1.1 cDNA.[10] Hox-1.3 probe was *Eco* RV-*Xba* I fragment of genomic Hox-1.3 gene.[11] Hox-2.4, 2.3 and 2.1 probes were *Bam* HI-*Kpn* I, *Bgl* II-*Bam* HI and *Eco* RI-*Xho* I fragments of the genomic Hox-2 cluster, respectively.[12-14] The *Eco* RI site of the Hox-2.1 probe was created by the *Eco* RI linker at 2.1 kb upstream of *Xho* I site during cloning. The homeodomain was removed from these probes except from Hox-2.4. Human β-actin promoter probe was human β-actin 14T-β-21 allele,[15] which has an extensive homology with the rat counterpart.[16] The probe was labeled to high specific activity[17] using a random primer oligolabeling kit (Boehringer Mannheim GmbH, Mannheim, Germany).

Northern blot analysis Total cellular RNA was extracted as described.[18] Then 10 μg of RNA was denatured, run through 1% formaldehyde gels and blotted onto filters.[6] The molecular probes used were RSV-LTR and the hamster α-tubulin gene.[19]

Immunoprecipitation Cells labeled with [^{35}S]methionine were immunoprecipitated with tumor-bearing rabbit serum (TBR)[20] essentially as described,[21] electrophoresed through 10% polyacrylamide gels[22] and fluorographed.

RESULTS

Polymorphism of cloned XC cells When XC cells were sparsely cultured to form colonies, some colonies consisted purely of thick, fusiform cells (L-type), and some others consisted purely of polygonal cells which were flat and displayed numerous "blebs" on the surface (R-type). The rest of the colonies could not be classified as L or R, because they were mixtures of the two types or they contained cells with intermediate morphology. The cells were cloned repeatedly to obtain pure cultures. We selected one clone for each type, L1 for L-type (Figs. 1A and 1C) and R1 for R-type (Figs. 1B and 1D). The distributions of actin and vinculin studied by fluorescence staining are shown in Fig. 2. Actin was observed as rosette-like structure both in L-type and in R-type cells and stress fibers were more conspicuous in R-type cells. Vinculin was detected as patches along the edge of R-type cells but not as such in L-type cells.

In order to examine whether these two cellular clones were derived from a single Rous sarcoma virus (RSV)-transformant, the high-molecular-weight DNA was extracted from L1 and R1, digested with Xba I (which cuts the genome of Prague C strain of Rous sarcoma virus at two sites[23]), electrophoresed, Southern-blotted, and hybridized with the RSV-LTR probe (Fig. 3B). The combination of the restriction enzyme and the probe used in this study gives us fragments which include a part of the viral genome and cellular flanking sequences. The hybridization pattern was identical in L1 and R1 (Fig. 3A). As the retrovirus integration site is random, the same hybridization pattern in the Southern blot analysis indicated that they were derived from the same transformed cell. There must be at least ten RSV proviruses in XC cells, since twenty bands were detected by the RSV-LTR probe.

In order to examine the stability of the morphology, L1 and R1 were replicated without cloning under a

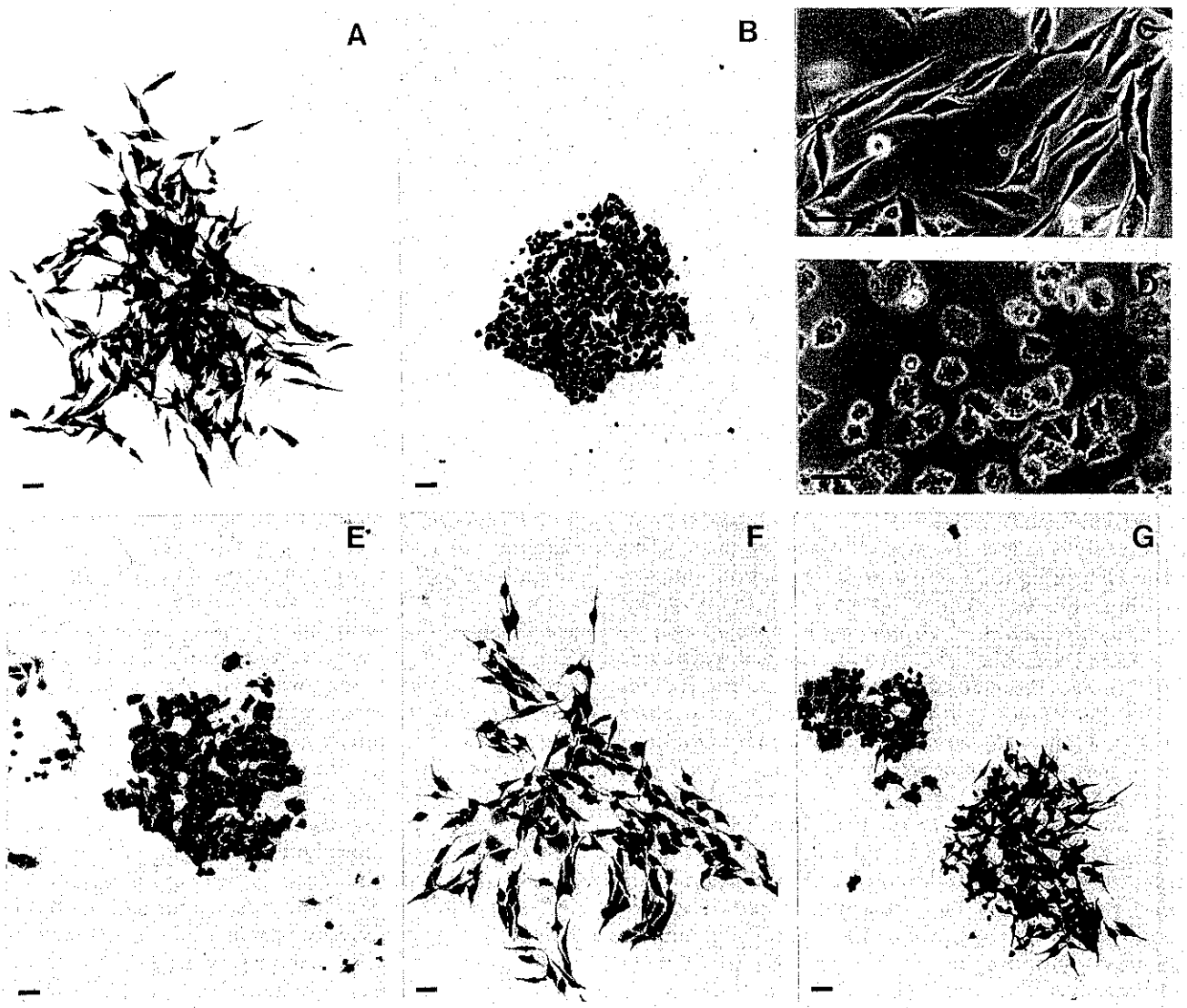

Fig. 1. Colonial and cellular morphology of L- and R-type XC clones. (A) L-type clone, L1. (B) R-type clone, R1. (C) Phase-contrast microscopy of L1. (D) Phase-contrast microscopy of R1. (E) R-type colony (LDR) which appeared in long-term culture of L1. (F) L-type colony which appeared in long-term culture of R1. (G) Co-culture of L- and R-type cells. Cells were fixed and stained with crystal violet for Figs. A, B, E, F, and G. Bar, 50 μm.

relatively strict schedule, i.e., subculturing 5×10^5 cells per 30×70 mm glass bottle every 4 to 5 days. At each subculture, the cells were plated in low numbers, 100 to 1000 cells per 60-mm Petri dish, to form colonies, and the fraction of L-type colonies was scored. As some colonies were mixtures of elongated and polygonal cells or those whose type was difficult to classify, only the typical L-type colonies were scored. The experiment was started about three weeks after the last colony isolation (time necessary for expanding the culture and for checking the purity of the clone). The population of L-type gradually decreased in the culture of L1, whereas it gradually increased in the culture of R1. The kinetics is shown in Fig. 4A. In either case, the percentage of pure L-type colonies stabilized at around 20%. This result could not be explained by insufficient cloning, since the stabilized phase consisting of the mixed population was attained starting from either L1 or R1. In addition, L1 and R1 had the same growth rate (Fig. 4B). An R-type cellular clone arising from L1 culture could be isolated (LDR) (Fig. 1E). The clone LDR was replicated without cloning; the population of L-type, which was less than 1%

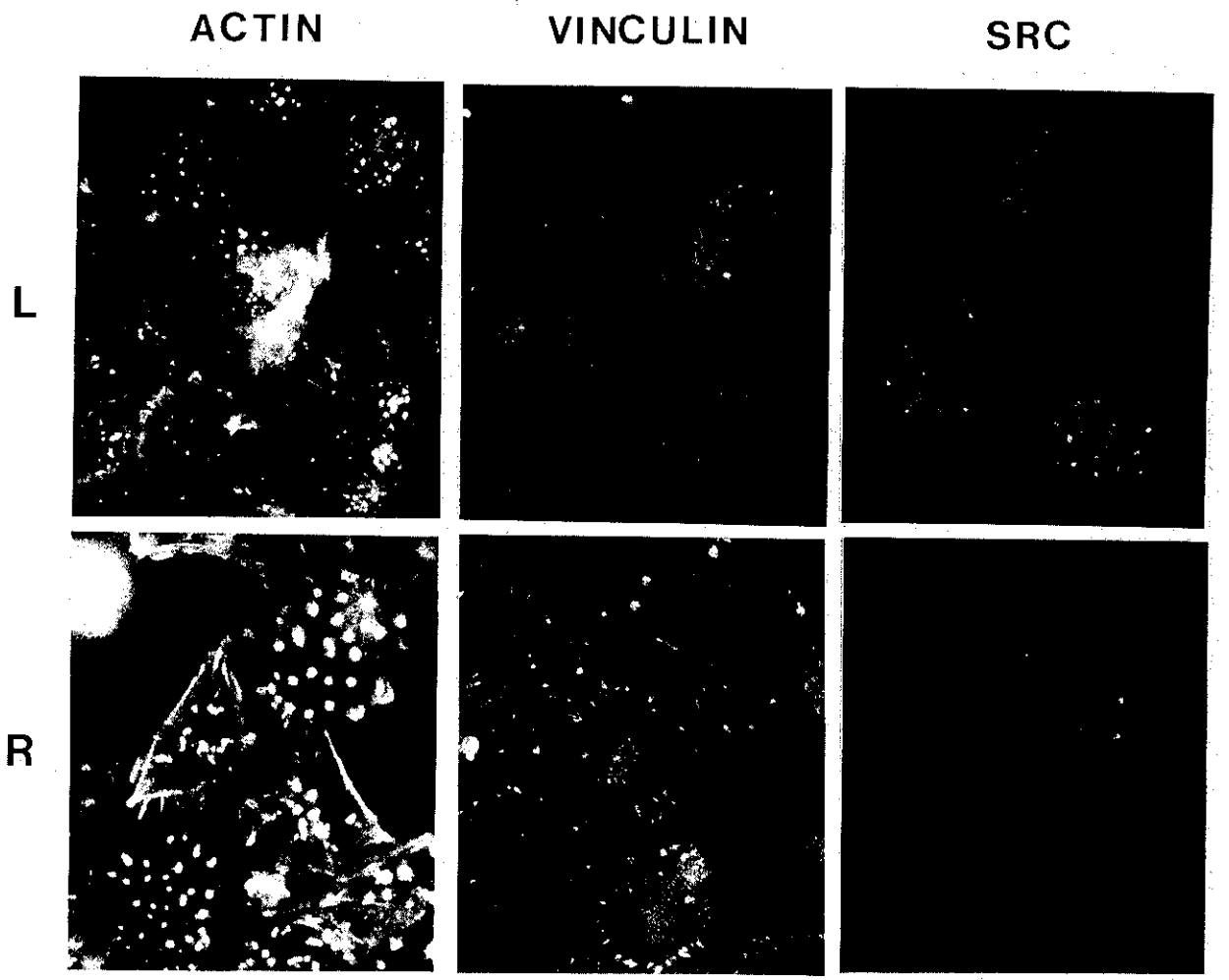

Fig. 2. Fluorescence staining of L- and R-type cells. F-actin was stained with rhodamine-conjugated phalloidin. Vinculin and $p60^{src}$ (SRC) were stained by means of the indirect immunofluorescence technique using monoclonal antibodies.

just after cloning, increased to 18% three months later. An L-type clone was also established from a long-term R1 culture (Fig. 1F). This observation firmly established a morphological conversion of XC cells. It is not likely that a soluble factor(s) was involved in determining the colony morphology, since typical L-type and R-type colonies grew side by side when they were co-cultured (Fig. 1G).

Conversion rate The kinetics of the conversion was sigmoid (Fig. 4A). This suggested that the morphological conversion consisted of multiple stages. If so, XC cells in the random culture must be at different stages of the conversion process. Consequently, the morphological stability of each single cell must be variable. In order to test this possibility, the following experiments were performed. Uncloned XC cells were plated in low numbers (20–30 colonies per 60 mm dish). Twenty well-separated colonies were isolated by the cylinder method and plated immediately in new 60-mm dishes. Ten days later the colonies derived from each clone were classified according to their morphology. Only the pure L-type colonies were scored. From the population of colonies produced, the original clones could be classified into three types, those producing L-type colonies in a minority (less than 2%), in a majority (more than 80%) and in intermediate numbers (Table I). The former two are relatively stable clones, and the last is a very unstable one. This experiment showed that the morphological stability was generally low and clonally variable. This is consistent with the multi-stepped process of morphological conversion mentioned above. Very stable lines could also be obtained. Subclones of L1 and R1, L1r and R1r

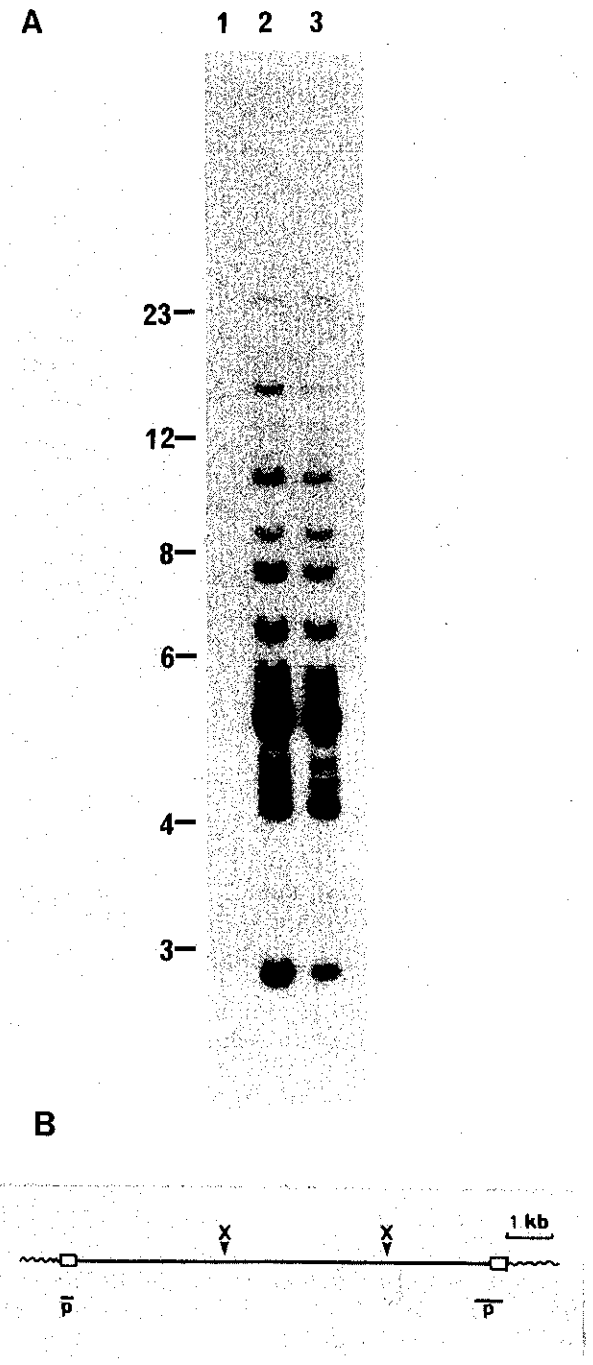

Fig. 3. (A) Southern blot analysis of chromosomal DNA of L- and R-type cells. Cellular DNAs from 3Y1 (lane 1), L1 (lane 2) and R1 (lane 3) were hybridized with RSV-LTR probe. (B) Schematic restriction map of the provirus (PRC strain of Rous sarcoma virus).[24] The solid line with the open boxes on both sides represents the provirus. The open boxes represent viral long terminal repeats (LTR). Wavy lines represent cellular flanking sequences. X indicates an *Xba* I site. Solid bars marked P show the area that the probe can hybridize.

respectively, remained morphologically pure for about 3 months. The following experiments for characterization of each clone were performed using these stable subclones.

Tumorigenicity on nude mice and colony-forming efficiency in semisolid medium In order to determine the tumorigenic potential of each cell type, L1r or R1r cells were inoculated into nude mice. The results of two such experiments are summarized in Table II. In Exp. 1, 1×10^7 cells were inoculated at a single site on the back of each mouse. All three mice inoculated with L1r cells developed large tumors in 14 days, while among the three mice inoculated with R1r cells, two did not develop the tumor at all, and only one developed a small tumor. In Exp. 2, the take was again higher for L1r than for R1r. Thus, L1r was more tumorigenic than R1r. Histologi-

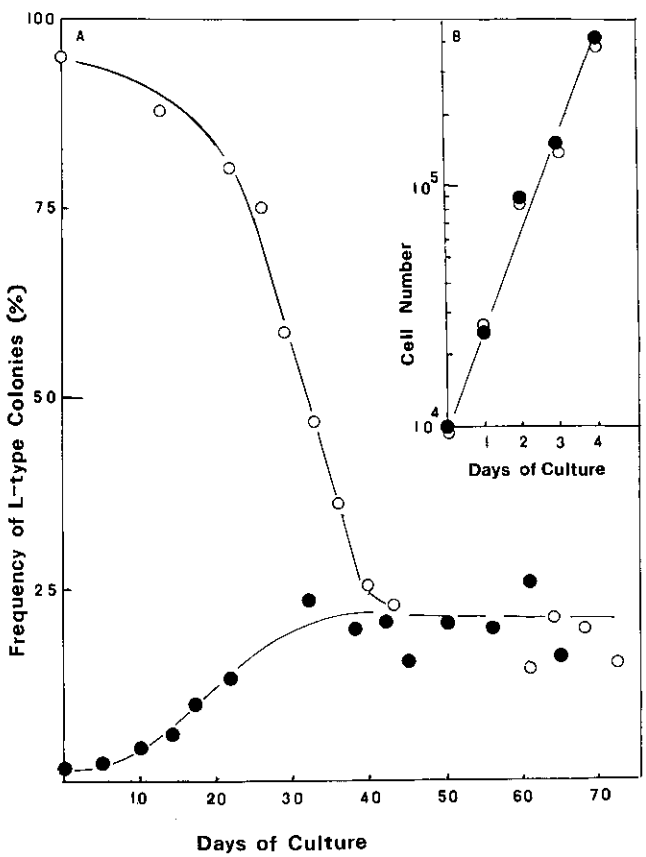

Fig. 4. (A) Degradation of pure L- or R-type clonal cultures into a mixture of both cell types. Frequency of L-type colonies (%) is plotted on the vertical axis, and days after the start of the experiment on the horizontal axis. Closed circles: R1. Open circles: L1. (B) The growth of L1 (open circles) and R1 (closed circles) clonal cells. Cell number is plotted on the vertical axis and the days of culture on the horizontal axis.

Table I. Different Frequencies of L-Type Colonies Produced from 20 Clones in the Equilibrium Phase Population

Colony	L-type	Non-L-type
1	0	125
2	0	34
3	0	11
4	0	196
5	0	134
6	1	126
7	1	48
8	1	156
9	1	168
10	30	12
11	29	19
12	31	57
13	37	7
14	46	7
15	67	6
16	81	6
17	58	8
18	113	9
19	8	0
20	167	0

Table II. Tumorigenicity in Nude Mice 2 Weeks after Inoculation

	No. of cells inoculated	Size of the tumors[a]	
		L1r	R1r
Exp. 1	1×10^7	$18\times11\times8$	$5\times3\times3$
	1×10^7	$20\times12\times9$	undetectable
	1×10^7	$22\times14\times12$	undetectable
Exp. 2	1×10^7	$14\times7\times5$	undetectable
	1×10^7	$10\times7\times3$	undetectable
	1×10^6	$5\times7\times5$	ND[b]
	1×10^6	undetectable	ND[b]

a) Size of the tumors is shown in mm.
b) ND, not determined.

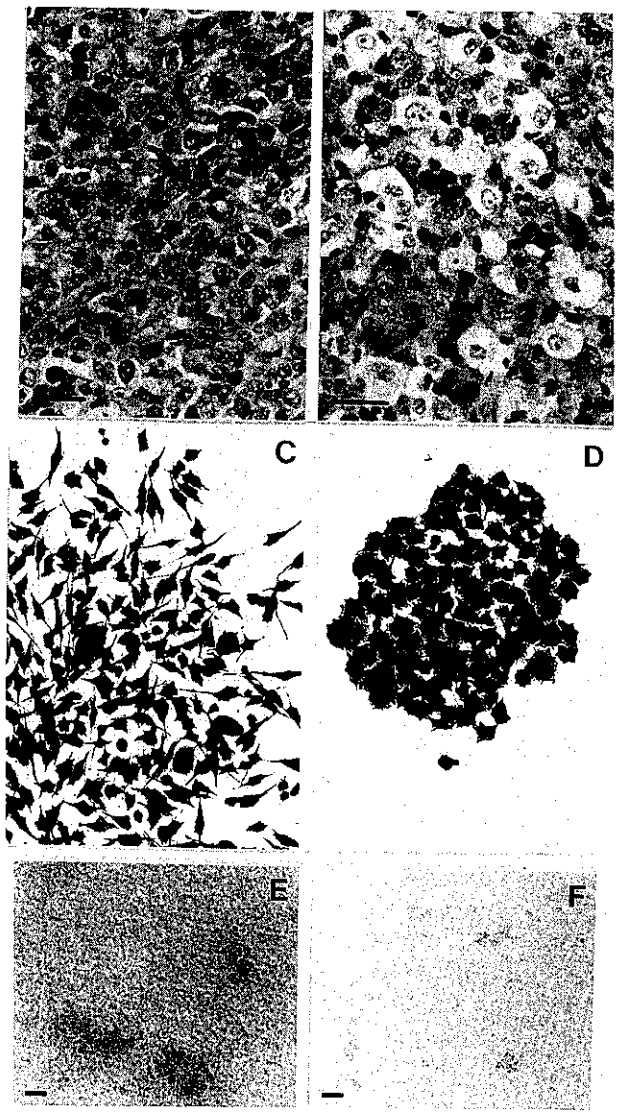

Fig. 5. Morphological features of the tumors induced in nude mice and on culture in methyl cellulose. Hematoxylin-eosin staining of tumors induced by L1r (A) and R1r (B). Bar, 25 μm. Colonies of cells recovered from tumors induced by L1r (C) and R1r (D). Methyl cellulose culture of L1r (E) and R1r (F). Bar, 50 μm.

cally, the tumors produced by L1r and R1r both consisted of round cells which resembled histiocytic tumor cells. But, the tumor cells of L1r were slightly smaller than those of R1r and had higher cellularity. In addition, the cells were uniformly basophilic in L1r tumors (Fig. 5A), while in R1r tumors, the cells with clear cytoplasm were present among those with basophilic cytoplasm (Fig. 5B). In order to examine the morphological stability during the tumor growth *in vivo*, the tumors were excised and the cells were cultured *in vitro*. As shown in Fig. 5C and D, the cells retained the original morphology.

When these XC clones were cultured in 0.8% methyl cellulose on the top of 1% agar, both L1r and R1r formed colonies. But, L1r formed much larger colonies than R1r (Fig. 5E and F). The colony-forming efficiency was 3% for L1r and 0.9% for R1r (colonies consisting of more than 10 cells were counted on day 21).

Expression of v-*src* gene products The above experiments showed that clonal XC cells underwent a morphological switch during culture, and the two clones had different tumorigenic potential. As the XC cells were originally transformed by RSV, it is possible that the morphological switch and the difference in the tumorigenicity were associated with the change in v-*src* gene expression. First, the transcriptional level of RSV genome was estimated by Northern blot analysis (Fig. 6A). When 10 μg of total RNA was hybridized with RSV-LTR probe, the most abundant message in XC cells was 21S mRNA (src message), in accordance with the published data.[24] In this exposure 38S mRNA could be seen faintly only in L1r and 28S mRNA could not be seen in either clone. Fig. 6B shows the same filter probed with the α-tubulin gene as an internal control. Densitometric analysis of the *src* message normalized with respect to the α-tubulin message suggested that the *src* message was about 3-fold higher in L1r than in R1r. The quantity of $p60^{v\text{-}src}$ was then estimated by immunoprecipitation of

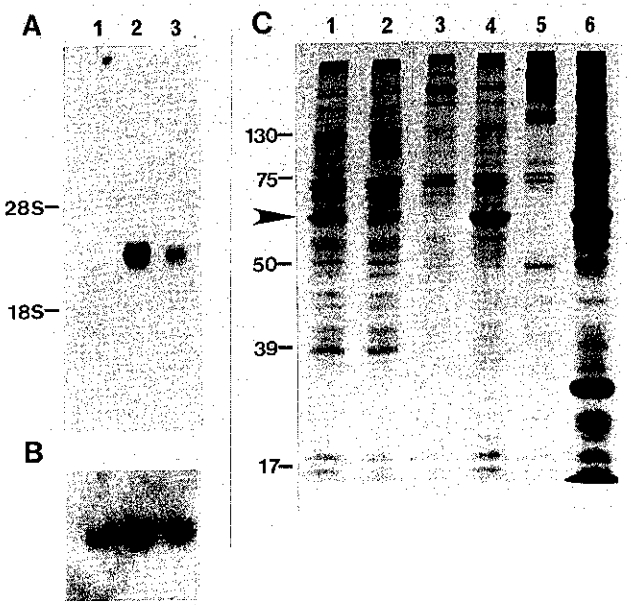

Fig. 6. RNA and protein expressions of v-*src* and *in vitro* kinase activity of $p60^{v\text{-}src}$. (A) Northern blot analysis of RSV transcripts with RSV-LTR probe. (B) The same filter was hybridized with α-tubulin probe as an internal control. Lanes: 1, 3Y1; 2, L1r; 3, R1r. Positions of 28S and 18S ribosomal RNA are indicated on the left. (C) Immunoprecipitation of cell lysates with TBR. Lanes: 1, L1r; 2, R1r; 3, 3Y1; 4, H21; 5, CEF; 6, CEF infected with SRA-RSV. $p60^{v\text{-}src}$ is indicated by an arrowhead. Molecular masses (in kilodaltons) are indicated on the left.

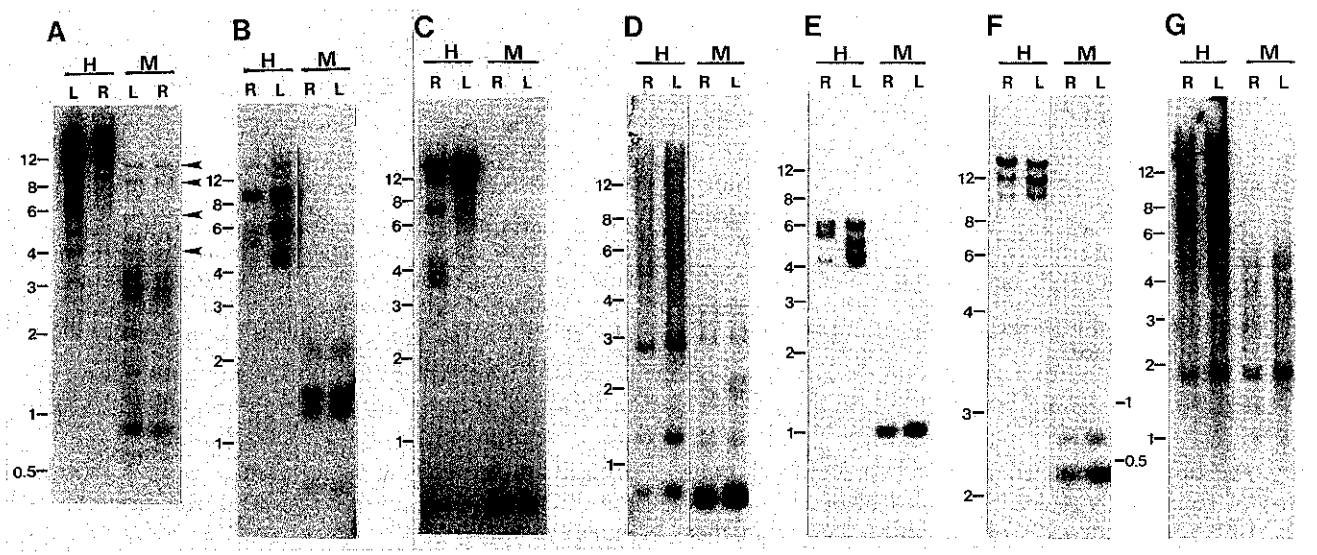

Fig. 7. Comparison of DNA methylation between L- and R-type cells. High-molecular-weight DNA from L1r (L) or R1r (R) was digested with *Hap* II (H) or *Msp* I (M) and was subjected to Southern blot analysis. Filters were hybridized with different probes. Probes: A, RSV-LTR; B, murine Hox 1.1; C, murine Hox 1.3; D, murine Hox 2.4; E, murine Hox 2.3; F, murine Hox 2.1; G, human β-actin promoter. A 1% agarose gel was used for electrophoresis except in the case of *Hap* II digest in F, for which 0.7% gel was used to get a better separation of large-molecular-weight DNAs. Molecular size (in kilobase pairs) deduced from a 1 kb DNA ladder (BRL, Gaithburg, MD) are indicated on the left of each figure.

[^{35}S]methionine-labeled cell lysates with TBR. [It precipitated $p60^{v\text{-}src}$ and other RSV products from RSV-transformed CEF (compare lanes 5 and 6 in Fig. 6C) and $p60^{v\text{-}src}$ from RSV-transformed rat cells (compare lanes 3 and 4 in Fig. 6C).] TBR precipitated $p60^{v\text{-}src}$ from both XC clones (though to a lesser extent than from transformed chick or rat cells). From L1r cells, about two-fold more $p60^{v\text{-}src}$ (by densitometry) was precipitated than from R1r (lanes 1 and 2 in Fig. 6C). Staining of L1r and R1r cells with anti-v-*src* monoclonal antibody (Fig. 2) revealed slightly more cytoplasmic fluorescence in L1r, in accordance with the results of immunoprecipitation (Fig. 6C).

DNA methylation as a possible mechanism The morphological type of either XC clone was stable for some time and then there was a switch from one type to the other. Even from relatively stable L1r and R1r, colonies with the opposite morphology appeared after a prolonged incubation (more than three months). The fact that the morphological conversion was reversible suggested an epigenetic process as an underlying mechanism rather than a structural change in DNA. DNA modification by cytosine methylation is a reversible change that can affect gene expression.[25] The state of DNA methylation in XC cells might be drifting and the cellular phenotype might be determined by activation of some gene(s). To examine the state of DNA methylation in L1r and R1r, we chose RSV-LTR and homeobox genes. The genomic DNAs from L1r and R1r were digested with *Msp* I or *Hap* II. *Msp* I cuts the tetranucleotide CCGG regardless of the methylation of the second cytosine residue, while *Hap* II cuts CCGG only when the second cytosine is unmethylated. The DNAs were probed with RSV-LTR, murine homeobox genes or human β-actin promoter (Fig. 7). As the RSV-LTR probe used had no *Msp* I/*Hap* II site and there is one such site in U5, the probe should detect two types of fragments, those spanning from the restriction site in the cellular flanking sequences to U5 in 5′-LTR, and the internal fragment spanning from the site in v-*src* to U5 in 3′-LTR. Although multiple fragments were detected in *Msp* I digests, the pattern was exactly the same in L1r and R1r (Fig. 7A). In *Hap* II digests, the majority of the bands migrated as high-molecular DNAs, suggesting that the sequences around LTR were heavily methylated in both clones. However, there was a distinct difference in methylation between the two clones. In R1r none of the *Hap* II fragments co-migrated with *Msp* I fragments, while in L1r there were several *Hap* II fragments which co-migrated with *Msp* I fragments (bands indicated by arrowheads in Fig. 7A). Thus, some proviral DNA methylated in R1r was demethylated in L1r.

As for homeobox genes, we chose the following murine probes, two from the Hox-1 cluster (Hox-1.1 and Hox-1.3) and three from the Hox-2 cluster (Hox-2.4, Hox-2.3 and Hox-2.1). The homeobox genes in mouse and humans are arranged very similarly in four clusters Hox-1, 2, 3 and 4.[26] Although information about the rat homeobox gene is limited, it appears reasonable to assume that the rat homeobox genes are also clustered and arranged similarly.[26] Hox-1.3 is located about 15 kb downstream from Hox-1.1 on mouse chromosome 6.[11] Hox-2.3 is located about 4 kb downstream from Hox-2.4 and Hox-2.1 is about 15 kb downstream from Hox-2.3 on mouse chromosome 11.[12] The cellular DNA was digested with *Msp* I or *Hap* II, electrophoresed and hybridized with one of these homeobox gene probes. As expected, the *Msp* I digest gave the same pattern for both clones, whichever probe was used (Fig. 7B–F). When the DNA was digested with *Hap* II, however, the bands detected by these homeobox gene probes migrated to higher positions than those digested with *Msp* I, and the positions of the bands were different between R1r and L1r clones except for the sample probed with Hox-2.1 (Fig. 7F). The results indicated that homeobox genes were methylated in both R1r and L1r, but the methylation pattern in these two clones was different in four out of five homeobox genes tested.

When the human β-actin promoter probe was used, *Msp* I and *Hap* II digests gave the same band in the two clones (Fig. 7G), suggesting that the β-actin promoter region was equally hypomethylated in these two clones.

DISCUSSION

Our experiments showed that clonal XC cells transformed by RSV could take thick, fusiform shape (L-type) or flat, polygonal shape (R-type). The two types were distinguished in terms of not only morphology but also tumorigenicity. Interestingly, the morphology was stable for some time, and then changed into the other morphology.

Rat cells transformed by RSV occasionally revert from the transformed state to the untransformed state, and less frequently transformed cells emerge from cells with the normal phenotype.[27] The reverted cells are morphologically indistinguishable from the normal cells and expression of virus-specific mRNA or its translation product is hardly detectable.[24, 27] As both L-type and R-type XC cells were transformants as judged by the anchorage independence, tumorigenicity and the presence of fairly abundant v-*src* gene products, the morphological conversion of XC cells is distinct from such transformation and reversion phenomena. Perhaps the difference in the morphology and tumorigenicity can be explained by the level of v-*src* gene expression. L-type, which expressed two- to three-fold more v-*src*, represents the morphology of more strongly transformed cells. Actually

a four-fold difference in cellular level of $p60^{v\text{-}src}$ produced differences in morphology and anchorage independence in rat cells.[28] In XC, expression of v-*src* must be controlled by an epigenetic process such as cytosine methylation. An inverse relationship between cytosine methylation and expression of proviruses has been reported,[29–32] and actually not only RSV proviruses but also cellular genes such as homeobox genes were differently methylated in L-type and R-type XC cells.

An alternative but less likely explanation is that L-type and R-type might express different $p60^{v\text{-}src}$. Temin showed that different RSV strains could transform cells to different morphological phenotypes.[33] A certain cloned virus stock induced round, refractile cells while other stock induced fusiform cells and so on. Fusiform morphology-inducing RSV often has lesions in the N-terminal half of $p60^{v\text{-}src}$.[34] One such fusiform mutant (d15) had a partial deletion in v-*src* gene and encoded a 52 kDa protein with tyrosine kinase activity,[35] while another mutant (CU12) encoded a protein with a molecular mass of around 60 kDa.[36] Anderson *et al.* also described an RSV mutant, CU2, which induces flat, nonrefractile, "blebby" morphology like that of R-type XC cells.[36] The reversibility of the morphological change and the rapid morphological conversion in XC cells cannot be explained by new acquisition of mutations such as those discussed above. It is possible, however, that XC cells harbor proviruses that underwent different mutations; one with CU12 type and the other with CU2 type mutations. Only CU12 type provirus might be expressed, while CU2 type provirus was shut off in L-type and *vice versa* in R-type cells. XC cells which express both types of provirus might take intermediate morphology. Again expression of the proviruses is controlled by an epigenetic process. This hypothesis can be tested by cloning and determining the primary structure of the v-*src* gene mRNA expressed in L-type and R-type XC cells.

ACKNOWLEDGMENTS

This work was supported in part by a Grant-in-Aid for Scientific Research and a Grant-in-Aid for Cancer Research from the Ministry of Education, Science and Culture of Japan, and by a Grant-in-Aid from the Ministry of Health and Welfare for the Comprehensive 10-Year Strategy for Cancer Control, Japan.

(Received December 6, 1990/Accepted March 9, 1991)

REFERENCES

1) Svoboda, J. The tumorigenic action of Rous sarcoma in rats and the permanent production of Rous virus by the induced rat sarcoma XC. *Folia Biol. (Prague)*, **7**, 46–60 (1961).
2) Kawabata, M., Yoshikura, H., Horio, K., Fujiwara, K. and Iwamoto, A. Clonal variation of adenylyl cyclase activity in a rat tumor cell line caused by change in G protein-catalytic unit interaction. *J. Cell. Physiol.*, **144**, 448–456 (1990).
3) Yoshikura, H., Naito, Y. and Moriwaki, K. Unstable resistance of G mouse fibroblasts to ecotropic murine leukemia virus infection. *J. Virol.*, **29**, 1078–1086 (1979).
4) Wulf, E., Deboben, A., Bautz, F. A., Faulstich, H. and Wieland, Th. Fluorescent phallotoxin, a tool for the visualization of cellular actin. *Proc. Natl. Acad. Sci. USA*, **76**, 4498–4502 (1979).
5) Chen, W-T. and Singer, S. J. Immunoelectron microscopic studies of the sites of cell-substratum and cell-cell contacts in cultured fibroblasts. *J. Cell Biol.*, **95**, 205–222 (1982).
6) Maniatis, T., Fritsch, E. F. and Sambrook, J. "Molecular Cloning: A Laboratory Manual," (1982). Cold Spring Harbor Laboratory, Cold Spring Harbor, New York.
7) Southern, E. M. Detection of specific sequences among DNA fragments separated by gel electrophoresis. *J. Mol. Biol.*, **98**, 503–517 (1975).
8) Gorman, C. M., Merlino, G. T., Willingham, M. C., Pastan, I. and Howard, B. H. The Rous sarcoma virus long terminal repeat is a strong promoter when introduced into a variety of eukaryotic cells by DNA-mediated transfection. *Proc. Natl. Acad. Sci. USA*, **79**, 6777–6781 (1982).
9) Yamamoto, T., Jay, G. and Pastan, I. Unusual features in the nucleotide sequence of a cDNA clone derived from the common region of avian sarcoma virus messanger RNA. *Proc. Natl. Acad. Sci. USA*, **77**, 176–180 (1980).
10) Kessel, M., Schulze, M., Fibi, M. and Gruss, P. Primary structure and nuclear localization of a murine homeodomain protein. *Proc. Natl. Acad. Sci. USA*, **84**, 5306–5310 (1987).
11) Fibi, M., Zink, B., Kessel, M., Colberg-Poley, A. M., Labeit, S., Lehrach, H. and Gruss, P. Coding sequence and expression of the homeobox gene Hox 1.3. *Development*, **102**, 349–359 (1988).
12) Hart, C. P., Awgulewitsch, A., Fainsod, A., McGinnis, W. and Ruddle, F. Homeo box gene complex on mouse chromosome 11: molecular cloning, expression in embryogenesis, and homology to a human homeo box locus. *Cell*, **43**, 9–18 (1985).
13) Krumlauf, R., Holland, P. W. H., McVey, J. H. and Hogan, B. L. M. Developmental and spatial patterns of expression of the mouse homeobox gene, Hox2.1. *Development*, **99**, 603–617 (1987).
14) Meijlink, F., de Laaf, R., Verrijzer, P., Destree, O., Kroezen, V., Hilkens, J. and Deschamps, J. A mouse

homeobox containing gene on chromosome 11: sequence and tissue-specific expression. *Nucleic Acids Res.*, **15**, 6773–6786 (1987).
15) Leavitt, J., Gunning, P., Porreca, P., Ng, S-Y., Lin, C. S. and Kedes, L. Molecular cloning and characterization of mutant and wild-type human β-actin genes. *Mol. Cell. Biol.*, **4**, 1961–1969 (1984).
16) Ng, S-Y., Gunning, P., Eddy, R., Ponte, P., Leavitt, J., Shows, T. and Kedes, L. Evolution of the functional human β-actin gene and its multi-pseudogene family: conservation of noncoding regions and chromosomal dispersion of pseudogenes. *Mol. Cell. Biol.*, **5**, 2720–2732 (1985).
17) Feinberg, A. P. and Vogelstein, B. A technique for radiolabeling DNA restriction endonuclease fragments to high specific activity. *Anal. Biochem.*, **132**, 6–13 (1983).
18) MacDonald, R. J., Swift, G. H., Przybyla, A. E. and Chirgwin, J. M. Isolation of RNA using guanidinium salts. *Methods Enzymol.*, **152**, 219–227 (1987).
19) Elliott, E. M., Sarangi, F., Henderson, G. and Ling, V. Cloning of 11 α-tubulin gene sequences from the genome of Chinese hamster ovary cells. *Can. J. Biochem. Cell Biol.*, **63**, 511–518 (1985).
20) Kawai, S., Yoshida, M., Segawa, K., Sugiyama, H., Ishizaki, R. and Toyoshima, K. Characterization of Y73, an avian sarcoma virus: a unique transforming gene and its product, a phosphopolyprotein with protein kinase activity. *Proc. Natl. Acad. Sci. USA*, **77**, 6199–6023 (1980).
21) Yoshida, M. and Yoshikura, H. Analysis of spleen focus-forming virus-specific RNA sequences coding for spleen focus-forming virus-specific glycoprotein with a molecular weight of 55,000 (gp55). *J. Virol.*, **33**, 87–596 (1980).
22) Laemmli, U. K. Cleavage of structural proteins during the assembly of the head of bacteriophage T4. *Nature*, **227**, 680–685 (1970).
23) Schwartz, D. E., Tizard, R. and Gilbert, W. Nucleotide sequence of Rous sarcoma virus. *Cell*, **32**, 853–869 (1983).
24) Quintrell, N., Hughes, S. H., Varmus, H. E. and Bishop, J. M. Structure of viral DNA and RNA in mammalian cells infected with avian sarcoma virus. *J. Mol. Biol.*, **143**, 363–393 (1980).
25) Holliday, R. The inheritance of epigenetic defects. *Science*, **238**, 163–170 (1987).
26) Kappen, C., Schughart, K. and Ruddule, F. H. Two steps in the evolution of Antennapedia-class vertebrate homeobox genes. *Proc. Natl. Acad. Sci. USA*, **86**, 5459–5463 (1989).
27) Chiswell, D. J., Enrietto, P. J., Evans, S., Quade, K. and Wyke, J. A. Molecular mechanisms involved in morphological variation of avian sarcoma virus-infected rat cells. *Virology*, **116**, 428–440 (1982).
28) Jakobovits, E. B., Majors, J. E. and Varmus, H. E. Hormonal regulation of the Rous sarcoma virus *src* gene via a heterologous promoter defines a threshold dose for cellular transformation. *Cell*, **38**, 757–765 (1984).
29) Groudine, M., Eisenman, R. and Weintraub, H. Chromatin structure of endogenous retroviral genes and activation by an inhibitor of DNA methylation. *Nature*, **292**, 311–317 (1981).
30) Groffen, J., Heisterkamp, N., Blennerhassett, G. and Stephenson, J. R. Regulation of viral and cellular oncogene expression by cytosine methylation. *Virology*, **126**, 213–227 (1983).
31) Mathey-Prevot, B., Shibuya, M., Samarut, J. and Hanafusa, H. Revertants and partial transformants of rat fibroblasts infected with Fujinami sarcoma virus. *J. Virol.*, **50**, 325–334 (1984).
32) Searle, S., Gillespie, D. A. F., Chiswell, D. J. and Wyke, J. A. Analysis of the variations in proviral cytosine methylation that accompany transformation and morphological reversion in a line of Rous sarcoma virus-infected Rat-1 cells. *Nucleic Acids Res.*, **12**, 5193–5209 (1984).
33) Temin, H. M. The control of cellular morphology in embryonic cells infected with Rous sarcoma virus *in vitro*. *Virology*, **10**, 182–197 (1960).
34) Wyke, J. A. and Stoker, A. W. Genetic analysis of the form and function of the viral *src* oncogene product. *Biochim. Biophys. Acta*, **907**, 47–69 (1987).
35) Iwashita, S., Kitamura, N. and Yoshida, M. Molecular events leading to fusiform morphological transformation by partial *src* deletion mutant of Rous sarcoma virus. *Virology*, **125**, 419–431 (1983).
36) Anderson, D. D., Beckmann, R. P, Harms, E. H., Nakamura, K. and Weber, M. J. Biological properties of "partial" transformation mutants of Rous sarcoma virus and characterization of their $pp60^{src}$ kinase. *J. Virol.*, **37**, 445–458 (1981).